GTP Hydrolysis by Purified α-Subunit of Transducin and Its Complex with the Cyclic GMP Phosphodiesterase Inhibitor†

Bruno Antonny, Annie Otto-Bruc, Marc Chabre, and T. Minh Vuong*

Centre National de la Recherche Scientifique, Institut de Pharmacologie Moléculaire et Cellulaire, 660 route des Lucioles, F-06560 Valbonne, France

Received January 27, 1993; Revised Manuscript Received May 13, 1993

ABSTRACT: The single-turn GTP hydrolysis by isolated and soluble transducin has been time-resolved using a rapid flow filtration technique which takes advantage of the GTP-requiring detachment of transducin α-subunits (Tα) from photoactivated rhodopsin (R*). Illuminated rod outer segment (ROS) fragments to which holo-transducin is tightly bound are retained on a syringe filter that is washed continuously with a buffer containing no GTP. When the flow is switched to a buffer with GTP, TαGTP is specifically eluted and injected into a cuvette where GTP hydrolysis is monitored via the associated change in the Tα intrinsic tryptophan fluorescence. Low concentrations of GTP elute the complete pool of Tα from the filter-retained ROS fragments in less than 1 s. This directly demonstrates that, upon GTP loading, Tα becomes instantly soluble in physiological buffers (120 mM KCl and 2 mM $MgCl_2$). When all alone, Tα hydrolyzes its bound GTP in 21 ± 1 s (1/e time at 25 °C). Replacing chloride by other anions increases the GTPase rate by 2-fold. The K_{50} for chloride inhibition of GTPase is ~2 mM. Slower GTP hydrolysis is observed for cholera-toxin-modified transducin or when GTPαS (Sp) replaces GTP in the eluting buffer. No signal is observed when GTPγS is used. The GTPase rate is unaffected when TαGTP binds to the inhibitory subunit (PDEγ) of the cGMP phosphodiesterase (PDE), although this binding is fast and of high affinity. This suggests that in a more complete system, where transducin and PDE deactivations take less than 1 s, additional factor(s) must speed up the GTPase rate of Tα.

In vertebrate visual excitation, the heterotrimeric G-protein transducin (TαTβγ) plays an important dual role as it acts in both the activation and the deactivation of the transduction cascade (Stryer, 1986; Chabre & Deterre, 1989; Lagnado & Baylor, 1992). In the activation phase, photoexcited rhodopsin (R*) binds to inactive, membrane-associated holo-transducin (TαGDP–Tβγ) and promotes the release of GDP from the Tα-subunit. Rapid binding of GTP to the empty nucleotide site induces Tα to switch to the "active" TαGTP form which dissociates from Tβγ and R*. This activation of transducin by R* and GTP takes but a few milliseconds (Vuong et al., 1984; Bruckert et al., 1992). Unlike for other G-proteins, the GTP-bearing α-subunit of transducin is soluble. TαGTP binds to and turns on a cGMP-specific phosphodiesterase (PDE) by displacing the inhibitory γ-subunit (PDEγ) from the catalytic αβ-moiety (PDEαβ). The ensuing drop in the free cGMP level causes closure of the cGMP-gated cationic channels on the plasma membrane and hyperpolarization of the rod cell. The PDE remains active as long as Tα is in the GTP conformation and keeps PDEγ away from its inhibitory site on PDEαβ.

What must be done to deactivate this transduction cascade? At the very least, photoexcited rhodopsin must be quenched, the stimulated PDE must be reinhibited, and the cGMP level must be restored to its dark level. R* is quenched by the concerted action of rhodopsin kinase and arrestin. In the simplest scenario, active PDE is reinhibited when TαGTP hydrolyzes its bound GTP and allows PDEγ to regain the inhibitory site on PDEαβ. Upon closure of the cGMP-gated cationic channels, the intracellular free Ca^{2+} drops and a guanylate cyclase is stimulated to replenish the cGMP pool; this restored cGMP level is directly responsible for the reopening of the channels. In this scheme, a swift GTP hydrolysis by Tα plays a necessary, albeit not a sufficient, role. As shown by time-resolved microcalorimetric measurements of the PDE activity from bovine ROS fragments at physiological light levels, the phosphodiesterase turns off in 0.5 s, provided GTP hydrolysis is not prevented by using the hydrolysis-resistant analog GTPγS in lieu of GTP (Vuong & Chabre, 1991). This result is particularly relevant, as electrophysiologically, a light pulse-induced hyperpolarization transient lasts less than 1 s (Lagnado & Baylor, 1992). Thus, in a complete system where interaction with its natural partners such as PDE is possible, transducin seems capable of very fast GTP hydrolysis. In amphibian ROS, holo-PDE as well as bovine PDEγ has recently been suggested to accelerate the GTPase rate of transducin (Arshavsky & Bownds, 1992). There is thus a strong hint that the deactivation of transducin is modulated by its interaction with other components of the transduction cascade. Likewise, in the muscarinic system, phospholipase C-β1, the effector of $G_{q/11}$, stimulates the steady-state GTPase rate of the latter by 10–20-fold (Bernstein et al., 1992).

What is the intrinsic GTPase rate of Tα when it is not associated with any other component of the cascade? As for most other heterotrimeric G-proteins, the currently accepted value for this GTPase rate is not compatible with the fast electrophysiological turnoff, as it ranges from 2 to 10 GTP hydrolyzed per minute per transducin. These are steady-state rates obtained under conditions of full photoactivation of the rhodopsin pool to minimize the contribution of the R*-catalyzed GDP/GTP exchange to the total duration of the GTPase cycle. What is the rate-limiting step in this cycle? The hydrolytic process by Tα itself, or a post-hydrolytic step? This question can only be unambiguously resolved by quickly creating a transient, isolated population of soluble TαGTP

† This study was supported by a grant from the Human Frontier Science Program.

* To whom correspondence should be addressed. Telephone (33)93-95-77-78. Fax (33)93-95-77-10.

0006-2960/93/0432-8646$04.00/0

and following its fate through time as it hydrolyzes its bound GTP. With many G-proteins, such as G_i and G_o, spontaneous, receptorless GTP loading may be achieved in low Mg^{2+} where GTP hydrolysis is slowed down. The stable population of GTP-bearing G-protein thus obtained can then be induced to undergo synchronous GTP hydrolysis by quickly raising the Mg^{2+} level (Higashijima et al., 1987a). Such a simple protocol is unfortunately not possible with transducin, as its rate of spontaneous nucleotide exchange is extremely low (2.4×10^{-5} s^{-1}; Bornancin et al., 1993). Consequently, measurements of the intrinsic deactivation time of transducin have always relied on R* to catalyze GTP loading. Given the long lifetime of R* in vitro, cycling over is unavoidable, and most of these measurements were therefore steady-state in nature.

We have developed a fast-filtration technique with which TαGTP can be quickly separated from illuminated ROS fragments and injected into a fluorescence cuvette where its conformational change to the inactive GDP state can be followed. The technique is based on three observations: First, once its nucleotide site is emptied, transducin is tightly bound to R*, i.e., to illuminated ROS fragments, which can be easily retained on commercially available syringe filters. Second, such "trapped" transducin can be eluted with a GTP-containing buffer because TαGTP is soluble, even at physiological ionic strength. Third, the tryptophan fluorescence of Tα decreases dramatically (–40%) as the protein changes from the GTP to the GDP state (Higashijima et al., 1987b). Thus, the intrinsic deactivation time of transducin can be measured on a soluble population which is entirely isolated from all other components of the cascade. Moreover, components whose interaction with TαGTP is known, such as the inhibitory subunit of the cGMP phosphodiesterase (Otto-Bruc et al., 1993), can be added in the receiving cuvette, and any influence they may exert on the GTPase rate can be studied. When measured with TαGTP alone in the fluorescence cuvette, the deactivation of TαGTP is a single-exponential decay with $\tau = 20$ s. In the presence of PDEγ, which binds tightly to TαGTP, the deactivation kinetics are unchanged: In solution, interaction with PDEγ alone is not enough to influence the GTPase activity of bovine Tα.

MATERIALS AND METHODS

Fast-Filtration Apparatus: Fluorescence and Transmission Flow Configuration (Figure 1A). Thanks to their micrometer size, ROS fragments from bovine retina can be deposited on filters whose pore size (0.22 μm) and material (PVDF) are such that the membranes are reliably retained while any protein that gets solubilized from them is carried away by the washing buffer and transferred to a fluorescence cell. Illuminated bovine ROS fragments are deposited on a syringe filter (Millex GV, 25 mm diameter, Millipore S. A., Molsheim, France). This filter can be freely washed with a buffer of moderate ionic strength without Tα getting detached, for in the absence of nucleotides, holo-transducin binds strongly to R*. But if the identical flowing buffer contains GTP or an analog, Tα is solubilized and can be quickly carried away from the filter. Given this differential solubility of transducin, a judicious flow-filtration system can be devised to quickly form a population of TαGTP and separate it from the R*-bearing ROS fragments.

The inlet of the filter is connected via a manually-operated 2-way valve to either one of two syringes, one containing just buffer (syringe 1), the other containing the same buffer supplemented with a nucleotide (syringe 2). Both syringes are pressurized by regulated compressed air at a constant pressure of 4.5 bar (Millex filters can withstand 5 bar). The capacities of syringes 1 and 2 are 40 and 10 mL, respectively. The outlet of the Millex filter feeds into a 300-μL quartz fluorescence flow cell which resides in the sample compartment of a fluorimeter (Model RF-5000, Shimadzu Corp., Kyoto, Japan). The filtrate, after its transit through the fluorescence flow cell, can be recovered for later analysis. With a ROS deposit containing 200 μg of rhodopsin, the flow rate through the system is 1.2–1.5 mL/s at 4.5 bar. The tryptophan fluorescence of proteins which flow through the quartz cell is continuously monitored with excitation at 292 ± 2.5 nm and emission at 340 ± 15 nm; the acquisition rate is 10 samples/s with a time constant of 15 ms. As guanine nucleotides absorb at 292 nm ($\epsilon_{292} = 1800$ M^{-1} cm^{-1}), a UV-sensitive photodiode (Model UV-100, UDT Sensors, Hawthorne, CA) is used to monitor the excitation beam as it emerges from the fluorescence flow cell. This in-line absorption setup allows us to record the time course with which GTP enters into the flow cell and to correlate it with the entry of the eluted proteins as monitored by fluorescence. Electronic sensing of the manually operated inlet valve is also possible

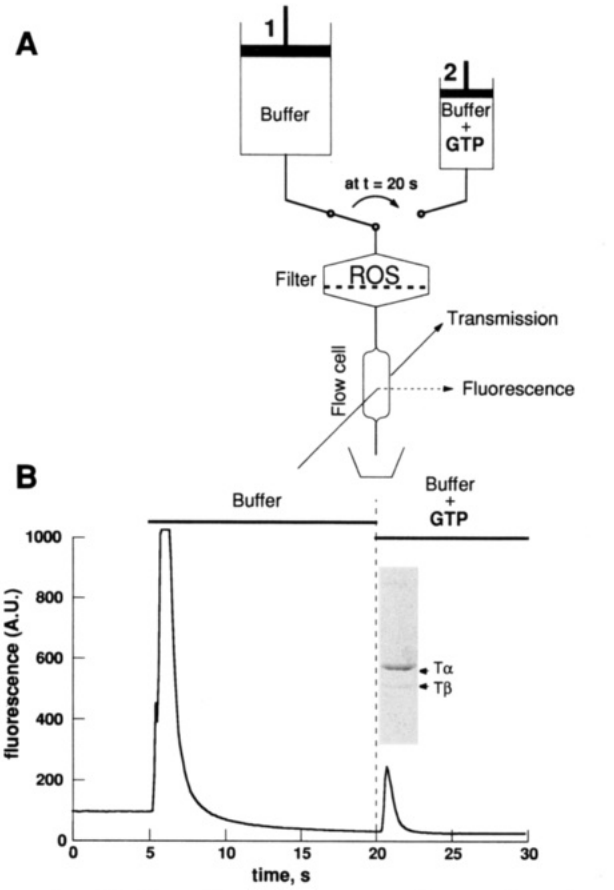

FIGURE 1: (A) Fast filtration apparatus, flow configuration. Illuminated bovine ROS are retained on a low-protein-binding PVDF syringe filter (Millex GV). Buffer and buffer + nucleotide are delivered with pressurized syringes 1 and 2, respectively. At 20 s, a manually operated 2-way valve is used to switch from an initial buffer wash to a buffer + nucleotide wash. Proteins eluted from the filter-retained ROS are injected into a 300-μL quartz flow cell, and their fluorescence is monitored. Absorption due to nucleotides is measured by monitoring the transmitted beam as it emerges from the flow cell. (B) Typical elution profile from illuminated ROS. ROS (200 μg of rhodopsin) are loaded onto the PVDF filter. The buffer wash is started at 5 s by turning on the air pressure. At 20 s, the 2-way valve is manually switched to commence the buffer + GTP wash. The fraction corresponding to the peak with GTP is collected and concentrated on Amicon-30, prior to analysis by SDS–polyacrylamide gel electrophoresis.

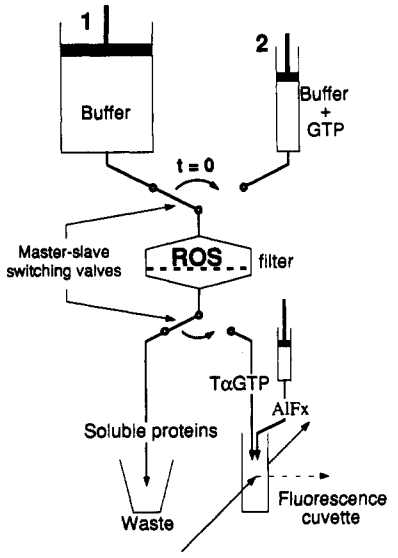

FIGURE 2: Fast-filtration apparatus, stopped-flow configuration. A 2-way solenoid valve is installed at the outlet of the syringe filter. This second valve is slaved to the manual 2-way valve via an optical proximity switch, which detects a reflector mounted on the piston of syringe 2. During the buffer wash, the solenoid valve diverts the filtrate to the waste. When the manual valve is switched to start the buffer + nucleotide wash, the solenoid valve is actuated after a suitable delay (~0.3 s) to direct the filtrate into a 1 × 1-cm quartz cuvette. As before, the illuminated ROS (200 μg of rhodopsin) are first washed for 15 s with buffer alone. At $t = 0$, the manual valve is flipped to start the buffer + GTP (or GTPγS) wash. The cuvette initially contains 700 μL of buffer (with or without PDEγ added), and the volume of the nucleotide filtrate injected into the cuvette is also 700 μL.

so that the exact instant of switching can be recorded by the data acquisition equipment. In a typical experiment, the Millex filter's inlet is first connected to syringe 1 so that the ROS sample can be washed for 15 s with buffer alone. Then the 2-way valve is manually switched to syringe 2, which contains the identical buffer plus a nucleotide. The first wash with buffer alone removes all weakly bound peripheral membrane proteins from the ROS fragments. The second wash is meant to release Tα from R* and carry it into the flow cell.

Fast-Filtration Apparatus: Fluorescence Stopped-Flow Configuration (Figure 2). The principle of operation is essentially the same as above except that the goal is not to monitor a flow of proteins but to collect the Tα filtrate into a standard 1 × 1-cm fluorescence cuvette so that its fate through time can be studied. In this configuration, the capacity of syringe 2 is only 1 mL, and pressurization at 4.5 bar is achieved with a set of calibrated weights. Again, before the value is switched over to the buffer + nucleotide wash, there is a 15-s wash with just buffer alone to remove all interfering, weakly bound peripheral proteins. This nucleotide-free filtrate is no longer fluorescently monitored but simply discarded. This calls for a more elaborate switching scheme with a 2-way solenoid valve mounted at the outlet of the Millex filter. With this additional valve, the flow can be diverted either to the waste during the 15-s buffer wash or to the cuvette during the buffer + nucleotide wash. When the inlet valve is switched to syringe 2 to commence the buffer + nucleotide wash, actuation of the outlet valve is delayed by about 0.3 s so that the 300-μL dead volume below the filter does not contaminate the fluorescence cuvette. To achieve this delay, an optical proximity switch which detects a reflector mounted on the piston of syringe 2 is used to control the outlet solenoid valve. Seven hundred microliters of filtrate is thus injected into the receiving cuvette, which already contains 700 μL of buffer (with or without proteins such as PDEγ added), so that the final sample volume is 1.4 mL. Vigorous stirring with a 6-mm magnetic stir bar ensures fast and complete mixing of these two volumes. The fluorescence cuvette is thermostated at 25 °C by a circulating water bath. Facilities are also provided for manual injections of sodium fluoride and aluminum chloride in the latter part of the experiment. Optical conditions for fluorescence monitoring are as before; the acquisition rate is 10 samples/s, but the time constant is now 0.125 s.

Preparation of ROS Samples. Fresh bovine eyes were obtained from a slaughterhouse. The ROS were prepared under dim red light as usual (Kühn, 1981) and stored at −70 °C until use. ROS pellets (1–2 mg of rhodopsin) were illuminated (30 s with orange light giving $R^*/R \approx 1$) and resuspended in isotonic HKM buffer containing 20 mM Hepes, pH 7.5, 120 mM KCl, 2 mM $MgCl_2$, and 1 mM DTT. The resulting suspension was divided into aliquots containing 0.2 mg of rhodopsin each; these were kept on ice in the dark. Before aliquots were deposited on the Millex filter, the volume of each aliquot was adjusted to 1 mL since the operation was carried out with 1-mL tuberculin syringes.

Buffers and Nucleotides. Syringes 1 and 2 were both loaded with isotonic HKM buffer (20 mM Hepes, pH 7.5, 120 mM KCl, 2 mM $MgCl_2$, and 1 mM DTT). The HKM buffer in syringe 2 also contained 50 μM GTP or an analog. GTPαS (Sp) was kindly provided by Dr. Fritz Eckstein. Concentrations of guanine nucleotides were determined by absorption spectroscopy ($\epsilon_{254nm} = 14\,000\ M^{-1}cm^{-1}$). The effect of chloride on the transducin GTP hydrolysis rate was studied by omitting Cl^- from the buffer. In this case, the ROS pellet was resuspended in a chloride-free starting buffer containing only 100 mM Hepes–NaOH, pH 7.5, and 2 mM $MgSO_4$. For each value of $[Cl^-]$, the buffer used for the 15-s wash and for eluting TαGTP was adjusted by adding the appropriate amount of KCl to the starting buffer.

Biochemical Assay of Eluted Transducin. The transducin-containing fractions of the filtrates from the flow experiments were collected and concentrated about 10-fold on Amicon-30 (W. R. Grace & Co., Beverly, MA) before being loaded on 12% SDS gels. The Coomassie blue stained bands were scanned densitometrically.

Preparation of PDEγ. The inhibitory subunit PDEγ was expressed as a native, nonfusion protein in *Escherichia coli* [see Otto-Bruc et al. (1993)] and purified essentially as described by Brown and Stryer (1989). When needed, it was added to the HKM buffer (700 μL) in the receiving cuvette of the stopped flow apparatus to give a final concentration of 200 nM.

Artificial Activation of TαGDP with AlF_x. NaF and $AlCl_3$ can impart on TαGDP an active conformation (Bigay et al., 1985; Antonny & Chabre, 1992). This is because there is binding of an AlF_3 ion at the β-phosphate of the GDP. Since AlF_3 mimics the γ-phosphate of GTP, the GDP thus partnered now behaves like a GTP and consequently confers upon the host G-protein the functionally as well as spectroscopically active GTP state. Thus, once TαGTP has hydrolyzed its GTP, the resulting TαGDP can be "reverted" to an artificial GTP state by injecting suitable amounts of NaF and $AlCl_3$ into the stopped-flow cuvette.

ADP Ribosylation of Transducin by Cholera Toxin. We used the protocol of Bornancin and Chabre (1991). Illuminated ROS fragments (0.2 mg of rhodopsin at 2 mg/mL) were incubated for 30 min at 30 °C in the presence of 75 μg/mL cholera toxin, 500 μM NAD, and 36 μM $GppCH_2p$

under continuous illumination with blue light (Kodak Wratten filter 48, λ_{max} = 460 nm) to promote photoreversion of metarhodopsin III. A control aliquot received the exact same treatment but for the omission of cholera toxin. The incubation buffer contained 200 mM NH_2PO_4, 12 mM arginine, 1 mM thymidine, 4 mM $MgCl_2$, and 10 mM DTT, pH 7. Following this treatment, the ROS fragments were directly deposited onto the Millex GV filter, and stopped-flow experiments were carried out as usual.

RESULTS

Fast Solubilization and Elution of Isolated TαGTP. A series of flow experiments were performed to test the overall validity of the principle of operation as outlined in Materials and Methods. The elution profile of one such experiment is shown in Figure 1B. The large first fluorescence peak is due to the weakly bound peripheral proteins ripped away from the ROS fragments by the vigorous 15-s buffer wash. There might also be included in this peak contributions from tiny ROS fragments which got squeezed through the 0.22-μm pores of the Millex filter. But by 20 s, this "contaminating" material was largely exhausted. When the buffer + GTP wash was initiated at 20 s, there appeared, after a slight lag, a second peak. After concentration on Amicon-30, this material was run on a 12% SDS gel; only two bands, which appear to correspond to Tα and Tβ, can be seen. Densitometry shows that the ratio of Tα to Tβ is about 7. As seen in Figure 3A, GTPγS is as efficient as GTP in eliciting this second peak at 20 s, while ATP is utterly without effect. In the run with ATP, the apparatus was slightly modified so a third wash with buffer + GTP could be accomplished after the buffer + ATP wash. While the buffer + ATP wash at 20 s elicited no peak, the subsequent buffer + GTP wash at 25 s resulted in a peak of amplitude and kinetics identical to those of the control peaks. When the GTP concentration was lowered from 50 to 0.3 μM, elution was retarded; the pulses in Figure 3B are seen to spread out more while retaining the same surface area. As the GTP level drops, there is a point below which one expects the entry of GTP into the emptied nucleotide site on Tα to slow down, thus delaying the dissociation of Tα from R*. This delay begins to be observable at about 3 μM GTP, while at 10 μM the elution kinetics are unchanged from those at 50 μM. This effect of low [GTP] on the elution profile parallels the findings of a detailed kinetic analysis of transducin activation performed with frog ROS (Bruckert et al., 1992): The bimolecular rate constant for the entry of GTP into the nucleotide site is $4.2 \pm 2.4 \times 10^7$ M^{-1} s^{-1}, and this entry becomes limiting when [GTP] drops below 20 μM. At 1 μM GTP, elution occurs in about 2 s (full width at half-maximum). This suggests a value of about 10^6 M^{-1} s^{-1} for the k_{on} of GTP in our case. The discrepancy between our estimate and that of Bruckert et al. (1992) resides perhaps in our using bovine ROS at room temperature. For all subsequent experiments, the GTP or GTPγS level was maintained at 50 μM so that nucleotide entry did not become limiting.

The arrivals of GTP and TαGTP into the flow cell were correlated as shown in Figure 3C. In an ideal system with infinitely fast response time, the GTP plateau should have been a perfect step function. Here, this step function is smeared to give a rise time of 0.7 s; this is the characteristic time of the instrument's impulse response, which we believe arises mainly from the dead volume of the filter chamber. The TαGTP elution peak also shows a full width at half-maximum of about 0.7 s, indicating that, with respect to our system, detachment of TαGTP from the ROS fragments is an impulse

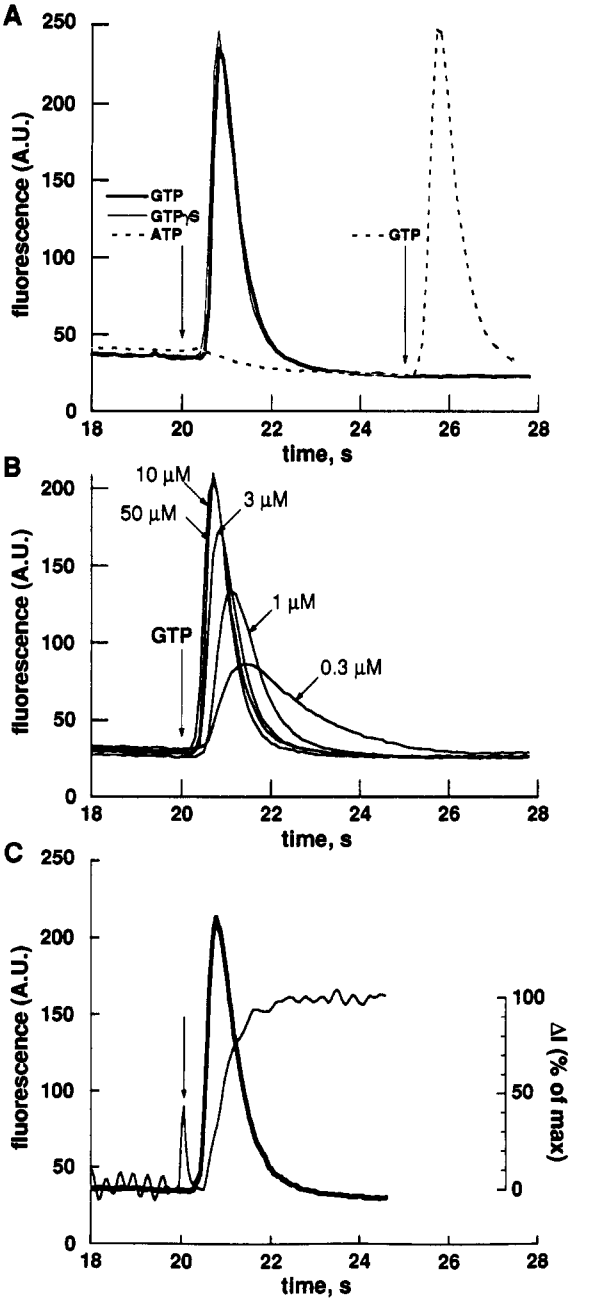

FIGURE 3: (A) Elution profiles with GTP, GTPγS, or ATP. Data are from the same experiment as in Figure 1B. Illuminated ROS (200 μg of rhodopsin) were sequentially subjected to a buffer wash between 5 and 20 s and then, between 20 and 25 s, to a wash with buffer + GTP (thick trace), buffer + GTPγS (thin trace), or buffer + ATP (dashed trace); the concentrations of all three nucleotides were 50 μM. For the experiment with ATP, a third wash was performed between 25 and 30 s with buffer + GTP. (B) Elution of transducin with varying levels of GTP. There was no observable difference in the elution kinetics between 10 and 50 μM GTP. Slowdown occurred at about 3 μM and was maximal at 0.3 μM. (C) Correlation between arrivals of GTP and transducin in the flow cell. The GTP level in the flow cell is monitored by the decrease of the transmitted light (thin trace), while the transducin level is monitored as usual by tryptophan fluorescence (thick trace); see Figure 1A. The small pulse (arrow) is an electrical signal which marks the switching of the manual 2-way valve.

function of width much less than 0.7 s. Formation of the TαGTP pool is thus quasi-instantaneous in the time range considered here. Results from these experiments (Figures 1 and 3) provide conclusive evidence that the protein peak elicited by the buffer + GTP (or GTPγS) wash consisted mainly of transducin α-subunit. Moreover, they directly and unequiv-

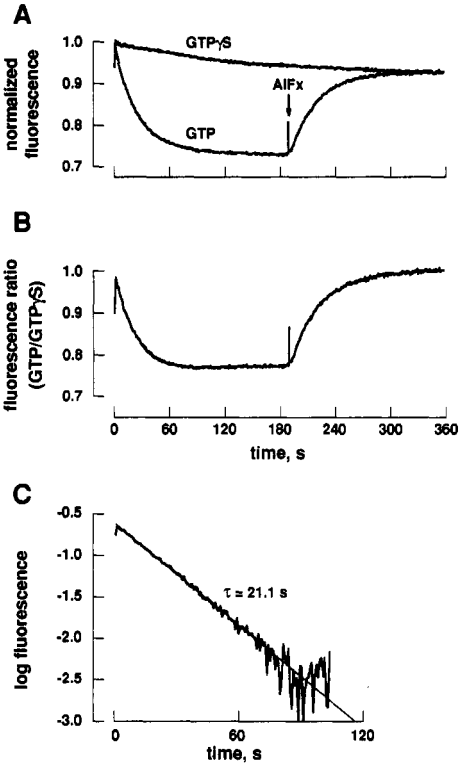

FIGURE 4: (A) Typical stopped-flow experiment. The illuminated ROS used contained 200 μg of rhodopsin; [GTP] and [GTPγS] were 50 μM. The GTPγS trace was normalized so that the fluorescence at time 0 is 1. The GTP trace is normalized to the GTPγS trace by using the values at 360 s. For the GTP trace, the fluorescence decay between 0 and 120 s corresponds to Tα deactivation upon GTP hydrolysis. Once this deactivation was completed, 5 mM NaF and 10 μM $AlCl_3$ were added (arrow) in order to artificially reactivate the resulting TαGDP (see text). The GTPγS trace shows only a slow drift which is due to T$\beta\gamma$ photobleaching and which parallels that of the GTP trace (see text). (B) Correction of the slow drift. This is done by simply computing the ratio GTP trace/GTPγS trace. The slow drift is effectively removed, yielding a stable GTP trace where AlF_x reversion results in a fluorescence level equal to that at time 0. (C) Characteristic time of GTP hydrolysis by isolated, soluble Tα. The semilog plot of the corrected GTP trace between 0 and 120 s is linear well over one decade and yields a rate constant for GTP hydrolysis of 0.05 s^{-1} corresponding to a time constant of 21 s.

ocally show that, in the GTP-bearing state, Tα is soluble in a buffer of near physiological ionic strength. With this fast-filtration technique, a soluble pool of TαGTP can be produced and almost simultaneously separated from the ROS membrane where the GTP loading took place.

Real-Time Measurement of the Intrinsic GTPase Rate of Isolated TαGTP. The intrinsic GTPase rate of isolated TαGTP was measured as shown in Figure 4. The filtration apparatus was operated in the stopped-flow mode; TαGTP eluted from the filter-retained ROS was injected at time 0 into the fluorescence cuvette. The tryptophan fluorescence of G-proteins in general and of transducin in particular is known to decrease in amplitude by 40% when the proteins undergo a conformational switch from the active, GTP-bound state to the inactive, GDP-bound state (Higashijima et al., 1987b). The fluorescence decay observed in Figure 4 between 0 and 180 s is due to this conformational change undergone by the Tα population that was injected into the fluorescence cuvette. The maximum amplitude of this decay was not 40%, as expected if only Tα were present; its lower value of 20% was due to the presence of the small amount of co-eluted T$\beta\gamma$ (see above, and Figure 1B). Indeed, Tγ is devoid of tryptophan, but Tβ contains eight residues, while Tα only has two. The contaminating population of T$\beta\gamma$ thus contributed a relatively constant fluorescence component which reduced the decay amplitude to 20%. Furthermore, when their fluorescence was monitored individually, purified T$\beta\gamma$ proved to be much more photolabile than TαGDP (data not shown). Thus, in addition to reducing the fluorescence change from 40% to 20%, the contamination by T$\beta\gamma$ also added a slight downward slope to the baseline, which can be seen once the GTPase-related decay is over (Figure 4A, GTP trace).

At 180 s, NaF and $AlCl_3$ (5 mM and 10 μM final concentrations, respectively) were manually injected into the cuvette. The subsequent fluorescence increase represents the reversion back to the GTP state of the TαGDP into which the original TαGTP had been transformed by GTP hydrolysis. This fluorescence increase is a rough measure of the concentration of TαGTP in the cuvette, which was 40–50 nM. Reversion with AlF_x did not yield a final fluorescence level equal to the one at time 0, as one would expect if the fluorescence drop at 180 s were due entirely to a GTP-to-GDP conformational switch undergone by Tα. This mismatch is yet another manifestation of the photobleaching of the contaminating T$\beta\gamma$. If the hydrolysis-resistant analog GTPγS was used in lieu of GTP, one would predict elution of Tα and some contaminating T$\beta\gamma$ in the usual proportion and no conformational switch by Tα, but photobleaching of T$\beta\gamma$ as always. This is indeed the case: The GTPγS trace of Figure 4A shows no marked decay between 0 and 100 s but only a continuous drift which parallels that of the GTP trace. Most significantly, when the GTP trace is normalized to the GTPγS trace using the fluorescence levels at 360 s, the levels at times 0 are seen to coincide. Hence, an obvious means to correct for the T$\beta\gamma$ photobleaching drift is to take the ratio GTP trace/GTPγS trace. As shown in Figure 4B, the thus corrected GTP trace is perfectly stable, and the fluorescence level, once reversion with AlF_x is over (300–360 s), is equal to the level at time 0. Therefore, in the experiment with GTP, the conformational change from TαGTP to TαGDP is entirely responsible for the decay between 0 and 120 s. Linearization of this decay (Figure 4C) shows that it is a single exponential with a lifetime of 21 s.

Four factors known to affect the GTPase rate of transducin were assessed (Figure 5). (i) When the hydrolysis-resistant analog GTPγS was used instead of GTP, the AlF_x-reversible fluorescence decay disappeared (see above). (ii) Once it was ADP-ribosylated by cholera toxin, Tα displayed a drastic slowdown in GTP hydrolysis. This decrease in GTPase rate is so severe that the long term (>20 min) drift of the fluorimeter prevented a reliable measurement of the asymptote of the fluorescence decay. A direct linearization of the ADP-ribosylated trace in Figure 5A was not feasible, and linearization had to be performed with the asymptote of the control trace (unmodified TαGTP). This yielded an estimated lifetime of about 200 s for cholera-toxin-catalyzed ADP-ribosylated TαGTP. (iii) When the Sp stereoisomer of the GTPαS analog is used instead of GTP, a single exponential decay with a lifetime of 73 s is observed, compared to 20 s for the control. Using the proton release technique to time-resolve the in vitro activation and turnoff of transducin-stimulated PDE, Yamanaka et al. (1985) reported that the deactivation rate of transducin decreases about 2-fold when GTPαS (Sp) is used instead of GTP. (iv) The Cl^- level in the buffer affects the GTPase rate; this confirms the findings of Higashijima et al. (1987c) for G_0. The lifetime of TαGTP steadily decreased as [Cl^-] in the buffer was reduced below 10 mM (Figure 5B). In the presence of 100 mM Hepes–NaOH, pH 7.5, 2 mM $MgSO_4$, and no Cl^-, the GTPase rate of transducin is about twice that of the control. The dose response for this Cl^- effect

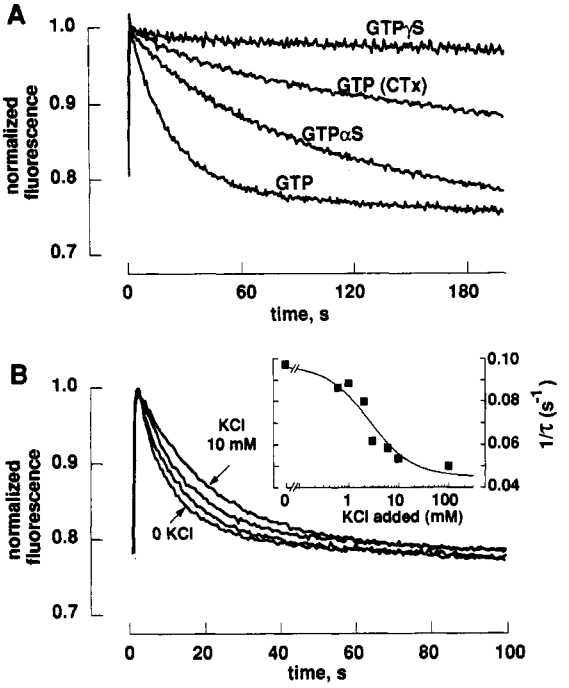

FIGURE 5: (A) Effects of GTPαS (Sp), GTPγS, and cholera-toxin-catalyzed ADP ribosylation of Tα on Tα GTPase activity. In all cases, transducin was eluted from illuminated ROS (200 μg of rhodopsin) with 50 μM of the indicated nucleotide. Transducin ADP ribosylation was perfomed as explained in Materials and Methods. (B) Effect of chloride on the GTPase activity of transducin. The experiments were performed as in Figure 4 except that the buffer contained 100 mM Hepes–NaOH, pH 7.5, 2 mM $MgSO_4$, 1 mM DTT, and varying concentrations of KCl. From the fastest to the slowest decaying curve, the concentration of KCl was 0, 0.6, 2, and 10 mM. Inset: Plot of the rate constant of GTP hydrolysis by Tα as a function of [KCl].

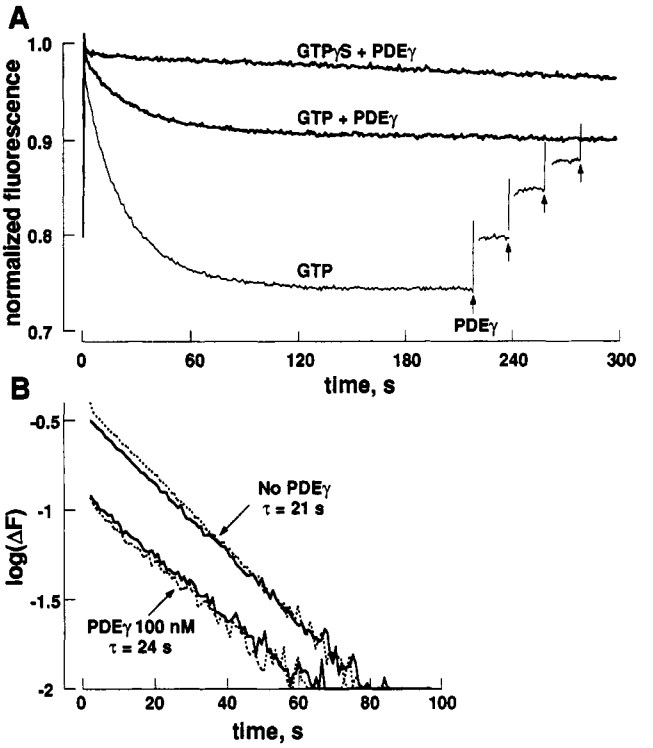

FIGURE 6: (A) Deactivation kinetics of the TαGTP–PDEγ complex. Upper trace, GTPγS + PDEγ, middle trace, GTP + PDEγ; lower trace, GTP only. In experiments with PDEγ, the receiving cuvette initially contained 200 nM PDEγ in 700 μL of HKM buffer. The volume of the filtrate injected into the cuvette was also 700 μL; thus the final PDEγ concentration was 100 nM. Given the affinity of PDEγ for Tα (see text), Tα molecules either in the GTP-, the GTPγS-, or the GDP-bearing form were associated with PDEγ at all times. Thus, for the middle trace, the fluorescence decay observed in the presence of 100 nM PDEγ monitors the GTP hydrolysis by the Tα–PDEγ complex. For the experiment with GTP alone, four aliquots of PDEγ (25 nM each) were manually injected (arrows) into the cuvette once the GTPase-related decay was over. The GTPγS + PDEγ and GTP + PDEγ traces were normalized so that their levels at time 0 were 1. The GTP trace was normalized to the GTP + PDEγ trace using the values at 300 s. (B) GTPase rates of Tα and Tα–PDEγ. Four stopped-flow experiments were performed on four ROS aliquots, two with 100 nM PDEγ present and two with no PDEγ added. The slopes of these linearized traces yield deactivation time constants of 24 ± 1 s with 100 nM PDEγ and 21 ± 1 s without PDEγ. All stopped-flow experiments were carried out with 50 μM nucleotides (GTP or GTPγS) and illuminated ROS corresponding to 200 μg of rhodopsin.

is shown in the inset of Figure 5, where the lifetime of TαGTP is plotted as a function of [KCl] in the buffer. It shows a 50% effect at ~2 mM KCl and saturation at 10 mM. The effect is specific for Cl^-. Similar results were obtained when KCl was replaced by another potassium salt, e.g., 60 mM K_2SO_4 (data not shown), instead of by Hepes–NaOH.

Search for an Effect of PDEγ on the GTPase Activity of TαGTP. Each TαGTP activates a cGMP phosphodiesterase by interacting with one of its two inhibitory subunits (PDEγ) and displacing it from one of the catalytic subunits (PDEα and PDEβ) (Deterre et al., 1988). There has been a slight controversy as to the exact molecular mechanism of this activation. When ROS are extracted with a low ionic strength buffer, TαGTPγS–PDEγ and active PDEαβ appear as soluble and separate species (Deterre et al., 1986; Wensel & Stryer, 1990). It was thus proposed that TαGTP activates the PDE by physically removing PDEγ from the still membrane-bound PDEαβ. It now appears that TαGTP binds to the membrane-associated holo-PDE and interacts with PDEγ, PDEαβ, and possibly with the membrane surface (Clerc & Bennett, 1992; Catty, et al., 1992). Activation results from PDEγ being displaced from PDEαβ but not from an outright removal. These clarifications aside, one can still say that TαGTP interacts with its effector mainly via binding to the inhibitory PDEγ subunit. We have shown (Otto-Bruc et al., 1993) that this binding also occurs in solution between soluble TαGTP and soluble PDEγ and that it is very fast ($k_{on} > 10^7\ M^{-1}s^{-1}$) and of very high affinity ($K_d < 0.1$ nM). PDEγ also associates rather well with TαGDP, the affinity being 2–3 nM. Thus, if there is enough excess PDEγ present, there will be no dissociation of TαGDP–PDEγ once GTP hydrolysis by TαGTP–PDEγ is over. Furthermore, just as with unpartnered Tα, TαGDP–PDEγ is also less fluorescent than TαGTP–PDEγ (Otto-Bruc et al., 1993). This difference in molar fluorescence and the swiftness with which TαGTP and PDEγ come together mean that GTP hydrolysis by TαGTP–PDEγ can also be time-resolved with our stopped-flow technique. Upon injection of TαGTP into the receiving cuvette, one may expect quasi-instantaneous formation of TαGTP–PDEγ, provided an excess of PDEγ is already present there.

Measurements of the deactivation rate of TαGTP–PDEγ are shown in Figure 6. The initial volume of buffer in the cuvette (700 μL) contained 200 nM PDEγ. After the 700 μL injected by the filtration setup was mixed in, the final PDEγ level was 100 nM. Given a $k_{on} > 10^7\ M^{-1}\ s^{-1}$ for the association between TαGTP and PDEγ, complex formation is expected to take less than 1 s. Since the Tα concentration was 40–50 nM, the free concentration of PDEγ should have been about 50 nM, which is much higher than the affinity of 2–3 nM between PDEγ and TαGDP. Hence, after GTP hydrolysis, the PDEγ–TαGDP complex remained as a single unit. Given

all these considerations, the GTP + PDEγ trace of Figure 6A must solely represent the deactivation of TαGTP–PDEγ; that is, the fluorescence decrease observed is due only to the conformational change undergone by the complex and not also to its post-hydrolytic dissociation. One notes that the amplitude of the decay recorded in the presence of PDEγ is smaller than in its absence (see GTP trace, Figure 6A). This is because the difference in molar fluorescence between TαGTP and TαGDP is larger than that between their PDEγ-complexed counterparts. Once the decay due to GTP hydrolysis was over, addition of PDEγ to the GTP control raised the fluorescence level to that of the TαGDP–PDEγ complex. The GTPγS + PDEγ trace again shows no GTPase-related decay but only a slow drift due to the photobleaching of T$\beta\gamma$.

The lifetime of the PDEγ–TαGTP complex can now be compared to that of TαGTP alone (Figure 6B). There is no significant difference in the slopes of the linearized traces, indicating that, in solution, TαGTP, whether alone or associated with PDEγ, is deactivated with the same characteristic time of about 20 s. Interaction with PDEγ does not speed up the GTPase activity of Tα; if anything, it seems to slow down this activity a little bit. This absence of effects by PDEγ persisted when chloride was either omitted from or replaced by sulfate in the buffer.

DISCUSSION

Using reconstituted systems containing only transducin (Tα and T$\beta\gamma$ in varying proportions) and photoexcited rhodopsin, steady-state measurements of phosphate release have yielded GTPase turnover numbers like 1 (Fung, 1983) or 1.6 GTP hydrolyzed per transducin per minute (Arshavsky et al., 1987). A quasi-real-time technique (Guy et al., 1990) consisted of monitoring the fluorescence change undergone upon injection of GTP by a suspension of vesicles incorporating R* and TαT$\beta\gamma$. There was first a fluorescence increase as Tα changed from the GDP to the GTP form. Then, upon exhaustion of the added GTP (by GTP hydrolysis), the fluorescence decayed as Tα returned to the GDP state after GTP hydrolysis. These are complex kinetic events. Strictly speaking, the fluorescence observed must be a convolution of two processes: the R*-catalyzed GTP loading (activation) and the GTP hydrolysis itself (deactivation). A rather involved model with several approximations was therefore needed to account for the observed fluorescence curves. Numerical fits of the data yielded a transducin deactivation time of 25–30 s. A common feature of all these experiments is that the process of transducin activation (i.e., R*-catalyzed GTP loading) could not be unequivocally separated from the process of deactivation (i.e., GTP hydrolysis). As a result, there has been a nagging suspicion that the steady-state measurements yielded such low GTPase turnover numbers because some step in the activation–deactivation cycle, other than GTP hydrolysis itself, is rate-limiting. But for its model-dependent conclusions, the work of Guy et al. (1990) tends not to support this hypothesis: The transition from TαGTP to TαGDP itself takes 20–30 s. Our rapid-filtration technique provides a means to physically segregate the process of activation from that of deactivation so that real-time recordings of the conformational change undergone by Tα as it hydrolyzes its GTP can be obtained. Our results clearly demonstrate that, at 25 °C, when solubilized and isolated from the rest of the transduction cascade, TαGTP is deactivated with first-order kinetics in 20 s (1/e time).

Is the fluorescence decay undergone by transducin strictly correlated with the breakage of the γ-phosphate bond? This question is important since Ting and Ho (1991) suggested that GTP hydrolysis by transducin is not limited by the cleavage of GTP, which would occur in 1–5 s, but by the slow departure of the inorganic phosphate. In such a model, clearly, if the fluorescence of transducin only reflected the presence of inorganic phosphate in the nucleotide site, measurements of these fluorescence changes would not kinetically reflect the first putative step of bond breakage. Moreover, any effects of PDEγ on this first step would also be missed. However, Guy et al. (1990) showed that the slow fluorescence decay of transducin (20–30 s) is strictly correlated with the production of total inorganic phosphate, including the hypothetical subpopulation that would still be in the nucleotide site. These results allow us to say with confidence that, contrary to the thesis of Ting and Ho, departure of inorganic phosphate is not rate-limiting and that even if transducin fluorescence changes only occurred upon this departure, they would still faithfully measure the hydrolysis of GTP. In addition, the experiments by Ting and Ho were performed using reconstituted bovine ROS. Analogous experiments using native ROS did not yield the same results (Pagès, 1993; F. Pagès and C. Pfister, personal communication).

The very fact that this technique of rapid filtration is possible provides incontrovertible evidence for the solubility of TαGTP in buffers of physiological ionic strength. Along with other biochemical (Kühn, 1980, 1981) and biophysical results (Kühn et al., 1981; Vuong et al., 1984; Bruckert et al., 1988, 1992), this direct demonstration should lay to rest the controversy about the solubility of TαGTP (Lamb & Pugh, 1992a,b; Liebman et al., 1987). The effect of low GTP concentrations on the elution of TαGTP from the ROS is in agreement with our light-scattering studies (Bruckert et al., 1992). The results reported here conclusively show that when [GTP] is lowered below $\sim$10 μM, the limiting step for the activation of transducin is the entrance of GTP into the open nucleotide site. Our results do not confirm an earlier conclusion by Kohl and Hofmann (1987), according to which the limiting step would be a conformational change by Tα.

Transducin deactivation times obtained with more physiological preparations and using a variety of techniques are significantly shorter than 20–30 s. In bovine ROS, when the PDE is activated following a light flash of physiological intensity (30 R*/rod), its turnoff requires GTP hydrolysis and takes a mere 0.5 s, indicating that deactivation of transducin is at least this fast (Vuong & Chabre, 1991). The single turnover method, when applied to amphibian ROS, yielded a transducin deactivation time of 1.7 s (Arshavsky et al., 1991). Faced with this dichotomy in the deactivation time of transducin, one is encouraged to think that there are factors in the intact system which accelerate the GTPase rate. One obvious candidate is the cGMP phosphodiesterase since physiologically, during its active lifetime, Tα is meant to be interacting with this enzyme. Indeed, recent experiments with amphibian ROS show that holo-PDE does stimulate the GTPase rate of Tα and, moreover, that even the inhibitory bovine PDEγ moiety is already capable of this stimulation (Arshavsky & Bownds, 1992). In the muscarinic system, Bernstein et al. (1992) have shown that the steady-state GTP hydrolysis by $G_{q/11}$ is stimulated 10–20 fold by its effector, phospholipase C-β1. Since we have demonstrated the fast formation of a very tight PDEγ–TαGTP complex in solution, it is natural to use our technique of fast filtration to further dissect this "GAP effect": Is interaction with just PDEγ sufficient to modify in some ways the GTPase activity of bovine Tα in solution? The answer is unequivocally no. Given the results from amphibian ROS, our negative findings suggest

some intringuing hypotheses. (i) In bovine rods, fast GTP hydrolysis requires interaction between TαGTP and holo-PDE on the membrane surface. (ii) Interaction with holo-PDE in itself is not enough to promote the GTPase activity of Tα but potentiates interaction with another protein component which does. Pagès et al. (1992) suggest that addition of exogenous holo-PDE to a suspension of bovine ROS fragments results in a doubling of the steady-state phosphate release rate. While providing some support for the former hypothesis, this result says nothing about the latter, as these ROS preparations contained the full complement of the transduction cascade.

We extend to transducin an observation made on G_0 by Higashijima et al. (1987c): Cl^- ions slow down the GTPase rate of transducin. From our dose-response curve this effect has a K_{50} of only 2 mM KCl. This raises the interesting possibility that the intracellular chloride level is an additional control point of the lifetime of active transducin, provided this quantity is well regulated in the retinal rod cell. However, the cytoplasmic level of chloride in ROS is currently not known with enough precision. Electrophysiological experiments on rod cells are carried out with "intracellular" buffers (when needed) containing 10–25 mM chloride. In other cells, the Cl^- level is reported to be between 5 and 15 mM (Albert et al., 1989).

ACKNOWLEDGMENT

We are grateful to Dr. Fritz Eckstein for the gift of GTPαS (Sp) and would like to thank Nordine Belmokhtar for skillful machine shop work.

REFERENCES

Albert, B., Bray, D., Lewis, J., Roff, M., Roberts, K., & Watson, J. D. (1989) In *Molecular Biology of the Cell*, p 301, Garland Publishing, Inc., New York and London.
Antonny, B., & Chabre, M. (1992) *J. Biol. Chem. 267*, 6710–6718.
Arshavsky, V. Yu., & Bownds, D. E. (1992) *Nature (London) 357*, 416–417.
Arshavsky, V. Yu., Antoch, M. P., & Philippov, P. P. (1987) *FEBS Lett. 224*, 19–22.
Arshavsky, V. Yu., Gray-Keller, M. P., & Bownds, D. E. (1991) *J. Biol. Chem. 266*, 18530–18537.
Bernstein, G., Blank, J. L., Jhon, D.-Y., Exton, J. H., Rhee, S. G., & Ross, E. M. (1992) *Cell 70*, 411–418.
Bigay, J., Deterre, P., Pfister, C., & Chabre, M. (1985) *FEBS Lett. 191*, 181–185.
Bornancin, F., & Chabre, M. (1991) *FEBS Lett. 291*, 273–276.
Bornancin, F., Franco, M., Bigay, J., & Chabre, M. (1992) *Eur. J. Biochem. 210*, 33–44.
Brown, R. L., & Stryer, L. (1989) *Proc. Natl. Acad. Sci. U.S.A. 86*, 4922–4926.
Bruckert, F., Vuong, T. M., & Chabre, M. (1988) *Eur. Biophys. J. 16*, 207–218.
Bruckert, F., Chabre, M., & Vuong, T. M. (1992) *Biophys. J. 63*, 616–629.
Catty, P., Pfister, C., Bruckert, F., & Deterre, P. (1992) *J. Biol. Chem. 267*, 19489–19493.
Chabre, M., & Deterre, P. (1989) *Eur. J. Biochem. 179*, 255–266.
Clerc, A., & Bennett, N. (1992) *J. Biol. Chem. 267*, 6620–6627.
Deterre, P., Bigay, J., Robert, M., Kühn, H., & Chabre, M. (1986) *Proteins: Struct., Funct., Genet. 1*, 90–99.
Deterre, P., Bigay, J., Forquet, F., Robert, M., & Chabre, M. (1988) *Proc. Natl. Acad. Sci. U.S.A. 85*, 2424–2428.
Fung, B. K.-K. (1983) *J. Biol. Chem. 258*, 10495–10502.
Guy, P. M., Koland, J. G., & Cerione, R. A. (1990) *Biochemistry 29*, 6954–6964.
Higashijima, T., Ferguson, K. M., Smigel, M. D., & Gilman, A. G. (1987a) *J. Biol. Chem. 262*, 757–761.
Higashijima, T., Ferguson, K. M., Sternweis, P. C., Ross, E. M., Smigel, M. D., & Gilman, A. G. (1987b) *J. Biol. Chem. 262*, 752–756.
Higashijima, T., Ferguson, K. M., & Sternweis, P. C. (1987c) *J. Biol. Chem. 262*, 3597–3602.
Kohl, B., & Hofmann, K. P. (1987) *Biophys. J. 52*, 271–277.
Kühn, H. (1980) *Nature (London) 283*, 587–589.
Kühn, H. (1981) *Curr. Top. Membr. Transp. 15*, 171–201.
Kühn, H., Bennett, N., Michel-Villaz, M., & Chabre, M. (1981) *Proc. Natl. Acad. Sci. U.S.A. 78*, 6873–6877.
Lagnado, L., & Baylor, D. (1992) *Neuron 8*, 995–1002.
Lamb, T. D., & Pugh, E. N. (1992a) *J. Physiol. (London) 449*, 719–758.
Lamb, T. D., & Pugh, E. N. (1992b) *Trends Neurosci. 15*, 291–298.
Liebman, P. A., Parker, K. R., & Dratz, E. A. (1987) *Annu. Rev. Physiol. 49*, 765–791.
Otto-Bruc, A., Antonny, B., Vuong, T. M., Chardin, P., & Chabre, M. (1993) *Biochemistry* (preceding article in this issue).
Pagès, F. (1993) *L'Activité GTPase de la Transducine dans les Bâtonnets Rétiniens de Bovins*, Doctoral Thesis, University of Grenoble I.
Pagès, F., Deterre, P., & Pfister, C. (1992) *J. Biol. Chem. 267*, 22018–22021.
Stryer, L. (1986) *Annu. Rev. Neurosci. 8*, 87–119.
Ting, T. D., & Ho, Y.-K. (1991) *Biochemistry 30*, 8996–9007.
Vuong, T. M., & Chabre, M. (1991) *Proc. Natl. Acad. Sci. U.S.A. 88*, 9813–9817.
Vuong, T. M., Chabre, M., & Stryer, L. (1984) *Nature (London) 346*, 659–661.
Wensel, T. G., & Stryer, L. (1990) *Biochemistry 29*, 2155–2161.
Yamanaka, G., Eckstein, F., & Stryer, L. (1985) *Biochemistry 24*, 8094–8101.